Agricultural and Forest Meteorology 306 (2021) 108445

Contents lists available at ScienceDirect

Agricultural and Forest Meteorology

journal homepage: www.elsevier.com/locate/agrformet

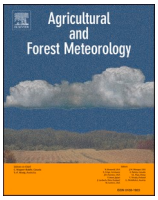

Assessing wine grape quality parameters using plant traits derived from physical model inversion of hyperspectral imagery

L. Suarez [a,b,*], P. Zhang [a], J. Sun [a], Y. Wang [b], T. Poblete [a], A. Hornero [c,d], P.J. Zarco-Tejada [a,b,c]

[a] School of Agriculture and Food, Faculty of Veterinary and Agricultural Sciences, University of Melbourne, Melbourne, Victoria, Australia
[b] Department of Infrastructure Engineering, Faculty of Engineering and Information Technology, University of Melbourne, Melbourne, Victoria, Australia
[c] Instituto de Agricultura Sostenible (IAS), Consejo Superior de Investigaciones Científicas (CSIC), Avda. Menéndez Pidal s/n, 14004 Córdoba, Spain
[d] Department of Geography, Swansea University, SA2 8PP Swansea, United Kingdom

ARTICLE INFO

Keywords:
Hyperspectral
Radiative transfer model
RTM
Nano-Hyperspec
Vineyards
Unmanned aerial vehicles
UAS
Wine aroma

ABSTRACT

Together with ensuring a stable yield, improving grape composition and aroma is the main goal of wine grape production management as it determines consumer acceptance and ultimately revenue. Understanding the triggers of the synthesis of aromatic components and finding methods to map their variability in the field can aid management practices during the season and planning selective harvest in views of maximizing benefit. Vegetation indices have been shown to track grape colour, sugar and acidity content but it has been demonstrated that aromatic components are the main drivers of the final palate of wine and are not correlated to sugar concentration. Leaf pigments such as chlorophyll, carotenoids and anthocyanins are involved in the metabolic pathways of aroma compounds in grapes. The physiological connections between grape aromatic components and primary and secondary photosynthetic pigments suggest that they could be used to detect processes related to aroma composition.

This study investigates the links between grape quality parameters such as aromatic components and image-quantified spectral indices and photosynthetic plant traits derived by physical model inversion methods. Two sets of high-spatial resolution hyperspectral and thermal imagery were collected with an unmanned platform at veraison and harvest. The variability found in the field was partly but not fully explained by the thermal-based crop water stress index as an indicator of water stress (r^2= 0.51–0.58, p-value<0.01). Fluspect-CX leaf model was coupled to 4SAIL canopy model and inverted to map the main photosynthetic pigment groups and the fraction of pigments acting in photoprotection. Results obtained through radiative transfer model inversion outperformed traditional vegetation indices related to pigment content and degradation. We found statistically significant relationships between image-retrieved pigments and terpenoids responsible for wine aroma (p-value<0.005).

1. Introduction

While ensuring a level of production is critical, wine grape managers also put their efforts on optimising grape quality, later resulting in better wine flavour. The flavour of a wine is the most important factor determining its consumer acceptance (Yegge and Noble, 2001), and this flavour is the result of a complex balance of all aroma components (Marais, 1983). While for other crops the benefit is mainly depending on yield and the management strategy is to maximise production, it is well known that for wine grapes the focus is on composition and over-cropping reduces grape quality, especially in cooler areas where it can lead to a delay in maturation and an increased susceptibility to disease (Stergios and Howell, 1977; Jackson and Lombard, 1993).

A high number of volatile components have been identified in grapes and wine contributing to the final flavour and a high proportion of those components are originating in the grape and then independent of the vinification process (Schreier, 1979; Black *et al.*, 2015). Most of these volatile or aroma components are terpenoids, secondary metabolites of diverse chemical composition (Yu and Utsumi, 2009; Mele *et al.*, 2020). Plants synthesise terpenoids as means of communication with other organisms through odour. They have the task of attracting pollinators or beneficial interactions (Suckling *et al.*, 2012; Muhlemann *et al.*, 2014) and deter pests (Boachon *et al.*, 2015). Apart from the interaction with other organisms, terpenoid synthesis is affected by sun exposure, water

* Corresponding author.
E-mail address: l.suarez@unimelb.edu.au (L. Suarez).

https://doi.org/10.1016/j.agrformet.2021.108445
Received 17 December 2020; Received in revised form 13 April 2021; Accepted 19 April 2021

availability and temperature (Gil *et al.*, 2013; Mele *et al.*, 2020). It is also function of vineyard management practices like defoliation or pruning which are used to improve final grape composition and quality (Jackson and Lombard, 1993; Hernandez-Orte *et al.*, 2014; Boss *et al.*, 2018). Terpenoids accumulate in grapes at different phenological stages but previous studies suggest that it is between veraison and harvest when the main synthesis activity takes place (Zhang *et al.*, 2016; Luo *et al.*, 2019).

The synthesis of terpenoids follows two main metabolic pathways where the major photosynthetic pigment groups are directly involved (Lichtenthaler, 1999). Like many terpenoids, carotenoids are isoprenoids and the chlorophyll molecule is isoprenoid-derived as well (Vranova *et al.*, 2012). Both terpenoid synthesis and leaf chlorophyll breakdown into secondary pigments have been linked to plant response to pest attacks (Peñuelas *et al.*, 1995). Some carotenoids are known to be affected by illumination intensity and act in photoprotection mechanisms to avoid oxidative damage and are direct precursors of some terpenoids like β-ionone (Bureau *et al.*, 2000a; 2000b). Both photosynthetic pigments and isoprenoids are involved in the same pathway which flux has been demonstrated to be highly affected by environmental and developmental factors (Vranova *et al.*, 2012). Although the full dynamics of this pathway have still not been thoroughly studied in plants, work done in seedlings showed how light intensity is one of the main regulators (Learned and Connolly, 1997; Šuklje *et al.*, 2014; Sasaki *et al.*, 2016). The understanding of the dynamics of the photosynthetic pigments is more advanced, including the effects of illumination intensity and stress on the pigment composition (Demmig-Adams and Adams, 1992; 1996; Matile *et al.*, 1999; Gilmore, 1997).

In order to adapt vineyard management practices toward the desired volatile synthesis level, there is a need for spatially explicit information on expected terpenoid concentration (Scarlett, *et al.*, 2014). Spectral-based remote sensing can provide the means to map this information. Previous studies have shown how remote sensing can assist vineyard managers with irrigation scheduling (Bellvert *et al.*, 2015), assessing the heterogeneity of pigment concentration (Zarco-Tejada *et al.*, 2013) or addressing nutrient deficiencies (Gil-Perez *et al.*, 2010; Meggio *et al.*, 2010). On the mapping of grape composition, most efforts have been put toward linking vegetation indices related to water (i.e. Serrano *et al.*, 2012, Gonzalez-Flor *et al.*, 2012) or nutrient stress (Meggio *et al.*, 2010) to grape sugar and acidity content. As an example, reflectance-based proxies of chlorophyll and carotenoids have been found to partially describe the grape composition and colour in tempranillo grapes (Martin *et al.*, 2007). Although the sugar and acidity content of grapes are important shaping the taste of the must, it has been demonstrated that it is the aroma or volatile components the ones driving the final character and palate of the wine. Those aroma components do not seem to be correlated to sugar concentration (Gonzalez-Barreiro *et al.*, 2015). Other studies have used indices related to plant growth and vigour to predict final grape composition (Lamb *et al.*, 2004; Hall *et al.*, 2010). These indices are a proxy of vegetation growth and health which can result in increased yield but not quality. As vine leaf area has been found to be inversely correlated to grape quality, methods based on vigour assessment can lead to wrong conclusions (Hunter *et al.*, 1991; Zhang *et al.*, 2017). To our knowledge, no studies are investigating the links between the synthesis of volatile components of the grape, indicators of grape aroma, and remote sensing derived photosynthetic pigment pools that are involved in the same metabolic pathways (i.e. chlorophylls and carotenoids).

There is extensive literature focusing on the estimation of photosynthetic pigments using spectral data (Blackburn, 2007; Zhang *et al.*, 2021). Pigment composition has traditionally been retrieved using spectral indices developed using specific wavelengths affected by specific absorption features. While accurate estimations can be achieved with vegetation indices, they are proxies of leaf pigment concentrations needing empirical relationships to establish those links, which are hardly universal across species, varieties and sites (Croft *et al.*, 2014). Vegetation indices are also affected by canopy structure, illumination intensity and soil background even when they have been optimized to minimise those confounding effects (Soares Galvao *et al.*, 2016). In vineyards, the estimation of both chlorophyll and carotenoid content has been demonstrated using high-spatial resolution hyperspectral imagery on pure vine pixels (Meggio *et al.*, 2010; Gil-Perez *et al.*, 2010; Zarco-Tejada *et al.*, 2013). These methods use vegetation indices in combination with radiative transfer models to minimise the illumination geometry, canopy structure and soil background effects on the spectral reflectance. Simulating the interaction of illumination and varying canopy structural scenarios and backgrounds adds computational complexity to the retrieval method but allows more robust and transferable results. Radiative transfer model inversion has also been used to simultaneously quantify several plant traits based on the full canopy spectrum (Jacquemoud *et al.*, 2009).

New advances in radiative transfer models now also provide the means to simulate plant photosynthetic and photoprotective activity adding new avenues to the remote sensing of stress to aid crop management (van der Tol *et al.*, 2009; Vilfan *et al.*, 2018). Vilfan *et al.* (2018) have updated the Fluspect-B model (Vilfan *et al.*, 2016) to simulate the xanthophyll composition changes to prevent the oxidative damage of photosystems under excessive illumination intensity. The new parameter C_x added in Fluspect-CX model represents the proportional fraction of carotenoids acting in photoprotection, allowing the simulation and retrieval of the xanthophyll cycle dynamics function of stress and directly involved in the synthesis of terpenes. Fluspect-CX combined with a canopy model like SAIL (Verhoef, 1984, Verhoef *et al.*, 2007) or similar enables the simulation of the main photosynthetic pigment groups and their photoprotection dynamics accounting for the structural effects of the canopy, permitting the retrieval of these plant traits through model inversion.

This work advances the current knowledge about the remote sensing of wine grape quality with views at aiding vineyard management and selective harvesting activities. Some of the key volatile components included in this study give a particular character to a variety or region when present, even in small concentrations (Black *et al.*, 2015). Although the final taste of must is the result of a combination of compounds and does not rely on individual molecules alone, establishing the links between remote sensing indicators and grape volatile components is the first step toward sensing and characterizing the full compositional matrix.

In this study, we explored the connections between photosynthetic pigment composition derived from airborne imaging spectroscopy and grape aromatic components measured at harvest. Hyperspectral and thermal imagery were acquired at veraison and harvest in a commercial vineyard (cv. shiraz) in Victoria (Australia). The low-altitude image acquisition provided a very high-spatial resolution which allowed the automatic extraction of pure vine spectral information. The main leaf pigment groups, along with the dynamics of the plant photoprotective mechanisms, retrieved through radiative transfer model inversion and traditional vegetation indices were related to grape volatile components at harvest. Finally, the crop water stress index (CWSI, Idso *et al.* 1981; Jackson *et al.* 1981) was used to assess the impact of water availability on the pigment variability and on the final grape quality.

2. Materials and methods

2.1. Study site and field data collection

This study was conducted in a commercial vineyard (Mount Langi Ghiran 37.31°S, 143.14°E) located at the base of two mount faces within the known as cool climate wine region (Gladstones, 2005). Five blocks of the variety shiraz were included in the study, where House Block 1-3 were oriented from northwest to southeast, House Block 4 was planted from east to west with vine spacing of 2.8 m between rows by 1.5 m between vines and the Old Block oriented from northeast to southwest at

Table 1
Platform and sensor operational settings during image acquisition.

Hyperspectral sensor characteristics and settings	
Spectral range	400 – 1000 nm
Number of spectral bands	260
FWHM	6.5 nm
Slit size	25 μm
Detector pixel pitch	7.4 μm
Focal length	4.8 mm
Radiometric resolution	12 bits
Integration time	18 ms
Thermal sensor characteristics	
Spectral range	7.5 – 13 μm
Resolution	640 × 480 pixels
Field-of-view (FOV)	45°
Focal length	13.1 mm
Radiometric resolution	16 bits
Image acquisition details	
Acquisition dates	22nd February & 17th April 2019
Flying height (above ground level)	100 – 120 m
Cruise speed	8 m/s
Mean spatial resolution	0.20 and 0.15 m/px respectively

a spacing of 3.0 m between rows by 1.8 m between vines. All grapevines were planted on their own root and trained to a vertical shoot positioned (VSP) trellis.

The soil type in the area is granite sandy on a clay loam sedimentary layer and the vines were irrigated with dripping irrigation lines installed along the rows. No significant pest and disease stresses were observed during the experimental season. Weather data was collected from the nearest Australian Bureau of Meteorology (BOM) weather station at Ararat Prison (BOM No. 089085) approximately 15.5 km northwest to the vineyard. The mean January, February, March maximum/minimum temperature recorded in vintage 2019 were 31.8/9.7°C, 27.9/9.4°C, 25.7/10.9°C, respectively. The monthly total rainfall in January, February, March were 1.2, 44 and 10.4 mm in vintage 2019 in comparison to the historical average (1969-2020) of 38.5, 31.6 and 29.6 mm indicating the dry January and March in the studied vintage.

A total of 43 monitoring blocks, each consisting of 3 rows of 4 vines were established in the summer of 2018-2019. 18 in the Old Block (OB), 16 in the House Blocks 1 to 3 (HB1-3) and 9 in the House Block 4 (HB4). Plots were selected to be homogeneous in structure (vine vigour) and leaf pigment content and representative of the spatial heterogeneity existing in the vineyard. Field data was collected in each of these blocks during veraison and harvest. Field measurements included stomatal conductance with a leaf porometer device (SC-1, Decagon Devices Inc., Pullman, WA, USA) measured on two fully exposed mature leaves and pigment concentration on a representative sample of 20 leaves per block using a Dualex instrument (FORCE-A, Orsay, France). At harvest, the monitoring blocks were harvested separately and taken to the laboratory for further analysis.

2.2. Airborne data collection

Within 4 days of field data collection, a nano-hyperspectral sensor (Headwall Photonics, Fitchburg, MA, USA) and a thermal camera (FLIR A655sc, FLIR Systems, Wilsonville, OR, USA) were installed on board an unmanned XM2 Tango platform designed and operated by XM2 Pursuit (Melbourne, Australia).

Flying operation was conducted along the solar principal plane at a

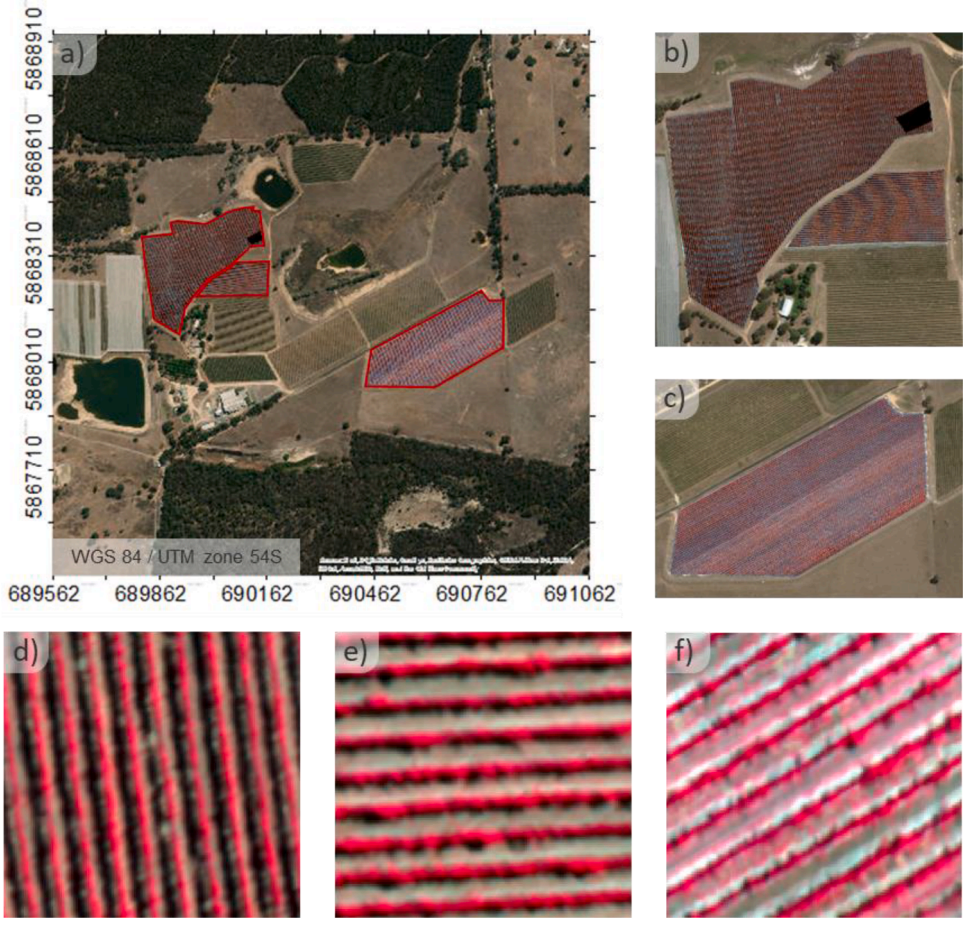

Fig. 1. False colour composite of the hyperspectral imagery acquired over Mount Langi Ghiran Shiraz House Blocks delineated in red (a). Zoom over House Blocks 1-3 (top) and House Block 4 (middle right) (b) and zoom over the Old Block (c). d-f) Close-up detail for House Block 1-3 (d), House Block 4 (e) and Old Block (f).

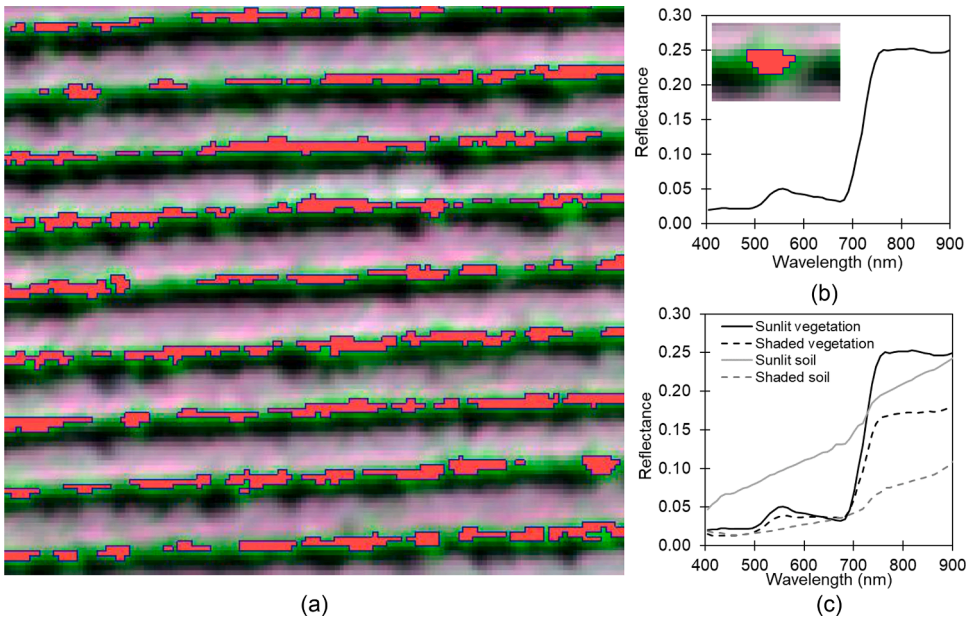

Fig. 2. Result of applying the automatic segmentation to an area with varying vine vigour (a), zoom over an individual vine and its corresponding spectrum (b) and spectra of the different scene components: sunlit vegetation, shaded vegetation, sunlit soil and shaded soil (c).

height between 100 and 120 m above ground level resulting in an average ground spatial resolution of 0.2 m for the hyperspectral and 0.15 m for the thermal imagery. Full description of the sensors and image acquisition details can be found in Table 1. Fig. 1 shows the location and extension of the Mount Langi Ghiran vineyard including the Shiraz blocks imaged for this study: House Blocks 1-3 (top) and House Block 4 (bottom, Fig. 1b) and the Old Block (Fig. 1c).

2.3. Assessment of grape and must composition

Eighteen Shiraz grape bunches were sampled from each of the labelled sampling location on the 3rd March 2019 before commercial harvest and transferred on dry ice to the University of Melbourne before stored at -20°C for future process. At each sampling location, Shiraz grape bunches were collected evenly from both sides of each row to achieve balanced sampling. Before laboratory analysis, all grape bunches were destemmed while frozen with stems, rachis, leaves, soil and insects removed. The remaining berries were stored at -20°C for future analysis. Prior to analysis, grape berry samples were sub-sampled to obtain representative samples. Grape pH, total soluble solids (°brix), titratable acidity (TA), relative total anthocyanins (520nm) and total phenolics (280nm) were measured using the standard protocol described by Iland (2004).

Terpene analysis was done using a headspace solid phase micro-extraction gas chromatography-mass spectrometry (HS-SPME-GC-MS) system. 50 g of representative grape berry samples were firstly sub-sampled and then ground into powder in liquid nitrogen to homogenise the resulting mixture of pulp and skin and prevent the loss of volatile components. 5 g of powdered grape sample was weighed into 50 ml tube, mixed with 30 ml of extraction buffer (5 g/l of TA, 5 g/l of PVPP, 0.5 g/l of sodium sulphite, pH 3.2) and shaken at 100 rpm for 24 h at 20°C in a temperature controlled incubator (ZWYR-240, Labwit Scientific, Ashwood, VIC, Australia). The tube was then centrifuged at 8000 g for 15 min and the supernatant was collected in syringe and filtered through a 0.45 μm nylon syringe filter (Thermo Scientific, Waltham, MA, USA). The filtered extract was collected in clean tube. All samples were prepared in triplicates.

Free terpenes and glycosidic bound terpenes were analysed separately following this step. For free terpene analysis, 5 ml of the filtered extract was transferred to a 20 ml GC sampling vials containing 1 g of sodium chloride and 20 μl of internal standard 4-octanol (10 mg/l in methanol) and sealed immediately. The samples were then subjected to GC-MS analysis described below. For bound terpenes, solid phase extraction (SPE) was performed using a C18 SPE cartridge (6 ml, 500 mg, Bond Elut, Agilent Technology, Santa Clara, CA, USA) as described previously (Zhang *et al.*, 2017). C18 column was activated with 10 ml of methanol, followed by 10 ml of milli-Q water at a rate of 1-2 ml/min. 30 ml of the clear grape extract from the previous step was passed through the activated column. Then, the column was rinsed with 10 ml of milli-Q water, followed by 10 ml of dichloromethane to eliminate sugars, acids and other free volatiles. The column was dried and eluted with 10 ml of methanol, and the eluate was collected in 20 ml GC sampling vials and dried under nitrogen gas to evaporate the methanol. The residual was then dissolved in 5 ml of citrate-phosphate buffer (0.1 M, pH 5) and 0.1 g of pectolytic enzyme was added to hydrolyse the glycosylated terpenes and shaken at 40°C for 24 h. 1 g of sodium chloride and 20 μl of internal standard 4-octanol (10 mg/l) was then added into the vial before GC-MS analysis.

Sample analysis was performed with an Agilent gas chromatography 6850 series II connected to an Agilent 5973 mass spectrometer (Agilent Technology) coupled with Agilent PAL multipurpose sampler. Separation was carried out using Agilent J&W DB-Wax ultra-inert column (30 m x 0.25 mm x 0.25 μm) with helium as carrier gas (99.999% purity, BOC, Adelaide, SA, Australia) at 0.7 ml/min constant flow rate. Polydimethylsiloxane/divinylbenzene SPME fibre (PDMS/DVB, 65 μm, Supelco, Bellefonte, PA, USA) was exposed to the headspace of the sample vial for 30 min at 40°C with agitation to extract volatile compounds. The SPME fibre was then desorbed at 220°C for 10 min in splitless mode. The oven temperature was set at 40°C for 4 min and increased to 160°C at 3°C/min, then increased to 230°C at 7°C/min and held at 230°C for 8 min. The temperature of mass spectrometer quadrupole, ion source and transfer line were set at 150°C, 230°C and 240°C, respectively. Mass spectrometer operated in positive EI mode at 70 eV with mass acquisition range of 35-350 m/z. A mixed alkane standard with a range of C7-C30 was analysed to calculate the retention index for each peak in the GC analysis. Terpenes in the sample were identified by comparing the terpene RI values and mass spectra to NIST library version 11 and that of authentic standards. Quantification was conducted by using standard calibration curves of a series of authentic terpene standards including α-pinene oxide, cis-pinane, 3-carene,

Table 2
List of spectral vegetation indices used in the study with their formulation and original reference. R_λ refers to reflectance at λ nm.

Index	Formulation	Reference
Blue Region indices		
NPQI	$(R_{415} - R_{435}) / (R_{415} + R_{435})$	Peñuelas *et al.* (1995)
BF_1	R_{400} / R_{410}	Zarco-Tejada *et al.* (2018)
BF_4	R_{400} / R_{440}	Zarco-Tejada *et al.* (2018)
Green Region indices related to carotenoids and photoprotection		
PRI	$(R_{570} - R_{530}) / (R_{570} + R_{530})$	Gamon *et al.* (1992)
PRI•CI	$((R_{570} - R_{530}) / (R_{570} + R_{530})) \cdot ((R_{760} / R_{700}) - 1)$	Garrity *et al.* (2011)
CAR	R_{515} / R_{570}	Hernandez-Clemente *et al.* (2012)
Chlorophyll content indices		
TCARI/OSAVI	$\frac{3 \cdot ((R_{700} - R_{670}) - 0.2 (R_{700} - R_{550}) \cdot (R_{700} / R_{670}))}{(1 + 0.16) \cdot (R_{800} - R_{670}) / (R_{800} + R_{670} + 0.16)}$	Haboudane *et al.* (2002)
LIC_3	R_{440} / R_{740}	Lichtenthaler *et al.* (1996)
RARS	R_{746} / R_{513}	Chappelle *et al.* (1992)
$PSSR_c$	R_{800} / R_{470}	Blackburn (1998)
Red-edge indices		
VOG	R_{740} / R_{720}	Vogelmann *et al.* (1993)
GM	R_{750} / R_{550}	Gitelson and Merzlyak (1997)
CI	R_{750} / R_{710}	Zarco-Tejada *et al.* (2001)
Structural indices		
NDVI	$(R_{800} - R_{670}) / (R_{800} + R_{670})$	Rouse *et al.* (1974)
RDVI	$(R_{800} - R_{670}) / (R_{800} + R_{670})^{0.5}$	Rougean and Breon (1995)
OSAVI	$(1 + 0.16) \cdot (R_{800} - R_{670}) / (R_{800} + R_{670} + 0.16)$	Rondeaux *et al.* (1996)

α-phellanderene, β-myrcene, α-terpinene, D-limonene, eucalyptol, β-trans-ocimene, γ-terpinene, p-cymene, o-cymene, terpinolene, rose oxide, theaspirane, linalool, terpinene-4-ol, β-cyclocitral, menthol, α-terpineol, nerol acetate, citronellol, β-damascone, geraniol, beta-ionone, thymol, trans-farnesol and cis-farnesol (Sigma-Aldrich, Castle Hill, NSW, Australia). The standard solution was serially diluted using PVPP buffer to establish the standard curves for free terpenes, and it was diluted using citrate-phosphate buffer to establish the second set of standard curves for bond terpenes.

2.4. Spectral data analysis

The hyperspectral imagery was radiometrically calibrated keeping the original instrument FWHM of 6.5 nm. Image raw data were transformed into radiance using calibration coefficients derived from measurements against a calibration standard (CSTM-USS-2000C LabSphere, North Sutton, NH, USA) at four integration times over four illumination intensities. The SMARTS model (Gueymard 1995; 2002) was used to conduct the atmospheric correction with the measurements collected with a handheld sun-photometer (Microtops II, Solar Light Co., Philadelphia, PA, USA) at the time of the flight and air temperature, relative humidity and air mass measured with a portable weather station (WXT530 Series from Vaisala, Vantaa, Finland). PARGE software package (ReSe Applications Schläpfer, Wil, Switzerland) was used to orthorectify each hyperspectral flightline based on the readings of an Inertial Measuring Unit (IMU) installed on-board the airborne platform during the flight (a full explanation of image calibration procedure can be found in Suarez *et al.*, 2021). Both the hyperspectral and thermal imagery were calibrated and pre-processed in the Laboratory for Research Methods in Quantitative Remote Sensing (QuantaLab) of the Spanish Council for Scientific Research (IAS-CSIC, Córdoba, Spain). For each block, pure vegetation pixels were selected from the imagery and averaged to compute the block spectral signal (Fig. 2).

An automatic segmentation process was conducted to extract the spectra corresponding to each vine over the whole area. Pure sunlit vine pixels were selected based on thresholds established using combinations of the reflectance at 580, 670 and 800 nm. The resulting segmentation together with a zoom over an individual vine with the corresponding spectral signal are shown in Fig. 2a and 2b. The surrounding spectral signal corresponding to shaded vegetation areas, sunlit and shaded soil is presented in Fig. 2c. Spectral indices traditionally used for vegetation stress detection were calculated using the average spectral signal corresponding to each block for both veraison and harvest acquisition times. The index selection comprises structural indices typically related to vigour and foliage density and indices used to assess pigment concentration and photoprotection mechanisms (Table 2). Indices linked to chlorophyll degradation calculated from bands in the blue region (Zarco-Tejada *et al.*, 2018) were added as the chlorophyll breakdown is an important catabolic process of fruit ripening and synthesis of volatile compounds (Hörtensteiner and Kräutler, 2011). For the image analysis, all blocks were used at veraison, when they were further grouped in homogeneous groups based on spatial proximity.

Table 3
Input parameter ranges used for FluSAIL.

Parameter	Definition	Unit	Range / Value
Leaf thickness and constituents			
N	Leaf structural parameter	[-]	1 – 2.5
C_{ab}	Chlorophyll a & b content	$\mu g/cm^2$	20 – 80
C_{car}	Carotene content	$\mu g/cm^2$	5 – 20
C_{ant}	Anthocyanin content	$\mu g/cm^2$	0 – 5
C_w	Leaf water content	g/cm^2	0.001 – 0.05
C_m	Leaf dry matter content	g/cm^2	0.001 – 0.05
C_s	Brown pigment content	$\mu g/cm^2$	0
Leaf dynamic biochemistry			
C_x	Proportional fraction of carotenoids acting in photoprotection	[-]	0 – 3
$f_{qe}I$	Fraction of photons partitioned to PSI	[-]	0.002
$f_{qe}II$	Fraction of photons partitioned to PSII	[-]	0.02
Canopy structural parameters			
LAI	Leaf area index	m^2 / m^2	0.3 – 5
q	Hot spot parameter	[-]	0.1
$LIDF_a$	Leaf Inclination Distribution Function parameter a	[-]	-1 – 1
$LIDF_b$	Leaf Inclination Distribution Function parameter b	[-]	-1 – 1

At harvest, four of the blocks were already in senescence and the image data from those blocks was not analysed, only points in the Old block that were still not harvested were used for further analysis.

The crop water stress index (CWSI) was also calculated as an indicator of water stress variability in the site. It was computed using the canopy-air temperature difference and the water vapour pressure deficit (VPD) measured at the time of the image acquisition (Idso *et al.* 1981; Jackson *et al.* 1981). For the upper and lower limits, the equations published by Bellvert *et al.* (2014) for wine grape cv. shiraz were used.

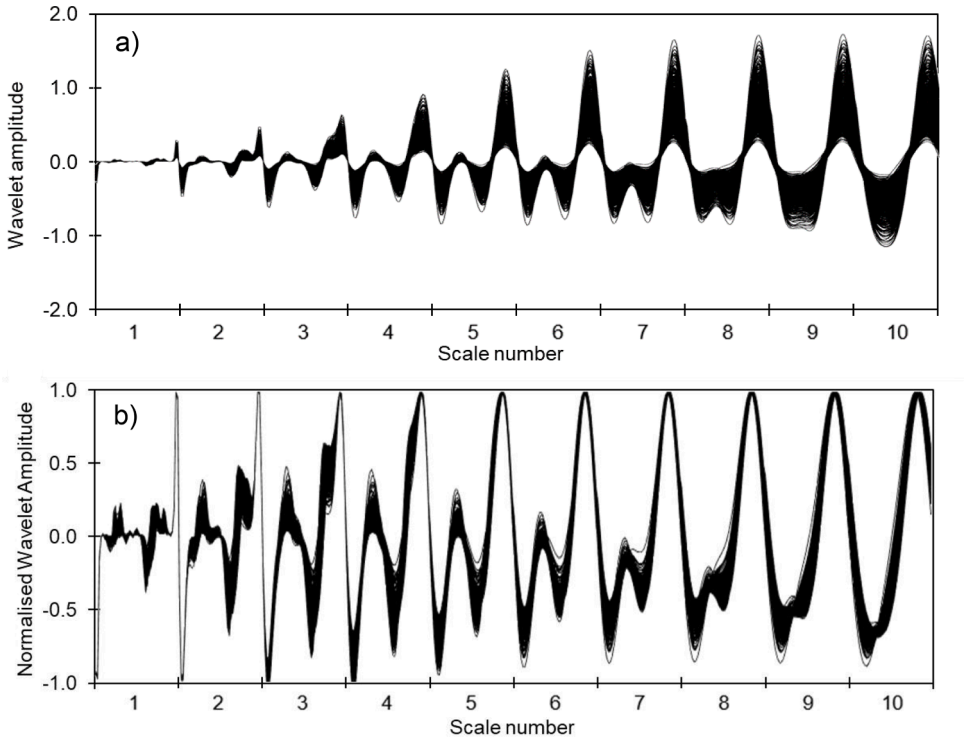

Fig. 3. Wavelet transform amplitude obtained for the whole range of input variation a) before applying any normalisation and b) after normalizing by dividing for the maximum of each scale.

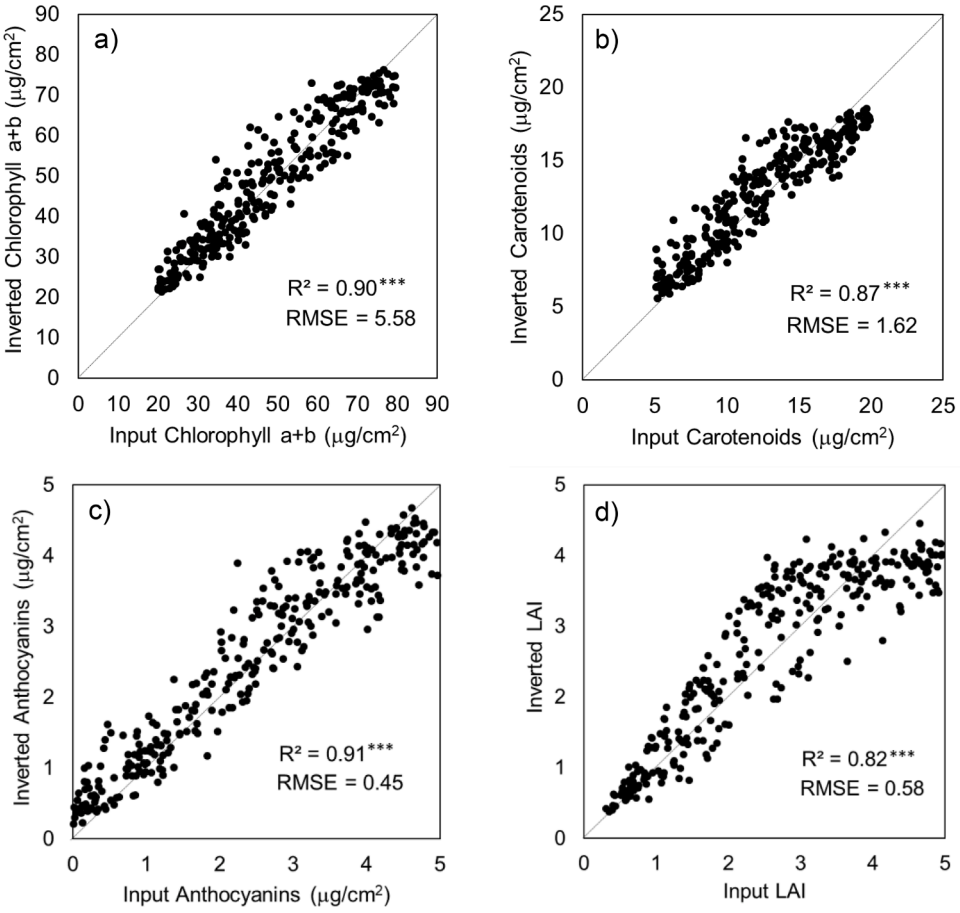

Fig. 4. Result of inverting the 3 main pigment pools and LAI using the wavelet inversion method with a synthetic LUT **p-value < 0.05; **p-value < 0.01; ***p-value < 0.001; n.s.=not significant.*

2.6. Radiative transfer model inversion of plant traits

Fluspect-CX model (Vilfan *et al.*, 2018) code was integrated with 4SAIL canopy code (Verhoef *et al.*, 2007) to create a coupled leaf-canopy model that allows the simulation of canopy reflectance for a range of biophysical and biochemical parameters presented in Table 3.

The reason of using the recently developed Fluspect-CX was to derive an indication of the epoxidation state (EPS) of the xanthophyll pigments together with the rest of pigments (chlorophyll, carotenoids and anthocyanins) included in previous Fluspect model versions (Vilfan *et al.*, 2016). We hereafter refer to the coupled leaf-canopy model as FluSAIL.

A 2-step inversion approach was undertaken to derive canopy biophysical and biochemical traits from image hyperspectral signal. A look-up-table (LUT) with 600,000 entries was generated using the full range of variation of the input parameters expected in a vineyard (see Table 3 for reference), illumination geometry at the time of the data capture and an average soil spectrum extracted from bare soil areas in the hyperspectral image.

The inversion was conducted based on wavelet transformed spectra. The use of wavelet transformation allows quantifying the magnitude of overlapping spectral features resulting from changes in canopy composition and functioning. This technique allows the analysis at different spectral scales, eliminating the confounding effects of both wide and narrow spectral features (Mittermayr *et al.*, 2001) and has been suggested as a method to minimise the effects of canopy structure when deriving pigment composition (Blackburn, 2006). This method has been used in the past to invert plant traits from hyperspectral imagery (Blackburn and Ferwerda, 2008; Cheng et al. 2011; Kattenborn *et al.*, 2017).

The second degree gaussian wavelet amplitude corresponding to each spectrum in both the image and the LUT was calculated for all spectral bands over 10 scales. As each plant trait has an effect on the spectral signal through features of different widths, all scales from 1 to 10 were used equivalent to characterising spectral feature widths between 9 and 90 nm. When using the wavelet transforms over the 10 scales, the amplitudes for each scale were normalised by dividing between the local maximum amplitude ($WVL_{\lambda,norm}$) as shown in Fig. 3.

This step avoided overfitting the inversion for the parameters affecting larger scales where the amplitude is higher in comparison to lower scales (Torrence and Compo, 1998). Fig. 3 shows the wavelet transformations of 300 simulations resulting from the full range of variation over the 10 scales, and the corresponding normalised spectra. All plant traits were retrieved as the average of the 50 closest $WVL_{\lambda,norm}$ entries in the LUT using the root mean square error (RMSE) as cost function.

Before applying it to the whole dataset, the methodology designed for this study was tested over 1000 simulations extracted from the 600,000 LUT corresponding to random inputs with a uniform distribution within the input ranges in Table 3. The theoretical results obtained for the main pigment groups and LAI are presented in Fig. 4.

A second inversion step was carried out to retrieve C_x. For each point, a new 500 entry-LUT was generated using the inputs retrieved in the first step and C_x varying fully from 0 to 3. Due to the localised and narrow effect of C_x in the spectra, only the wavelet amplitude calculated for the first three scales over the green spectral region was used to determine the closest simulation each image spectrum based on the root mean square distance. Inversion was conducted using a fraction of the spectrum previously determined by simulating the effect of C_x variation on the wavelet transform using the spectral sensor configuration (band centre and width).

The model inversion method was applied to the average signal of every vine extracted through the above-mentioned automatic segmentation. This allowed creating interpolated maps of chlorophyll content and the product $C_{car}\bullet C_x$ as an indication of the total carotenoids acting in photoprotection over the whole study site. The spatial interpolation, conducted for visualisation purposes was performed using the natural neighbour algorithm (Sibson, 1981).

Table 4
Overview of the leaf measurements acquired in the field between veraison and harvest.

Indicator	Mean	Minimum	Maximum	Standard deviation
Chlorophyll *a*+*b* (a.u.)	25.86	19.13	34.48	2.98
Flavonoids (a.u.)	2.20	2.05	2.41	0.06
Anthocyanins (a.u.)	0.16	0.13	0.21	0.02
NBI (a.u.)	11.79	8.79	15.76	1.35
g_s (mmol/m^2•s)	175.44	102.09	297.99	55.60

3. Results

3.1. Field and laboratory data

The analysis of the measurements conducted in the field demonstrates a high level of variability in pigment concentration and stomatal conductance (g_s) (Table 4). This variability could be partly attributed to a long-term effect of the water availability differences in an undulated terrain with a sandy upper layer. This is demonstrated with the significant correlation found between chlorophyll content measured in the field and the difference between canopy and air temperature (T_c-T_a) (Fig. 5).

3.2. Link between remote sensing indicators and grape composition

The radiative transfer model inversion based on wavelet transforms of the pure vine spectra yielded a good spectral fit for all blocks (Fig. 6) indicating the robustness of the methodology presented.

The Pearson coefficients obtained for the relationships between grape compounds (Table 5) and different vegetation indices extracted from the hyperspectral image at veraison are presented in Table 6. All the indicators based on leaf pigment composition and pigment degradation showed a strong significant correlation with major terpenes in free form responsible for the final grape and wine aroma (p-values $<$ 0.01). Weaker relationships were found between structural indices related to vigour and vine growth like NDVI or RDVI. No significant correlations were found when comparing grape composition parameters with spectral indices calculated from the imagery collected at harvest (data not shown).

Indicators quantified through model inversion outperformed spectral indices yielding stronger correlations with a wider range of grape volatile compounds (Table 7). Chlorophyll content derived through model inversion shows the best predicting potential for free terpene composition overall. Spectral indices typically used for chlorophyll content estimation like TCARI/OSAVI, although highly correlated, did not present the same strength (Fig. 7). Both leaf chlorophyll *a*+*b* and carotenoid content derived from model inversion at veraison present a negative correlation with terpenes like terpinolene and limonene but a positive correlation with linalool (Table 7 and Fig. 7). The opposite is found for anthocyanins which are positively correlated to terpinolene and limonene but show an inverse correlation with linalool. α-Terpineol and linalool were found to be more related to the carotenoids composition and the proportion of xanthophyll pigments acting in the photoprotective processes function of stress both in relative (C_x, r^2= 0.64; p-value = 0.002) and absolute terms ($C_{car}\bullet C_x$, r^2= 0.71; p-value = 0.001). PRI, as a spectral index developed to track xanthophyll composition changes, showed a trend (r^2= 0.45; n.s.) although not statistically significant (Fig. 8). No statistically significant relationships were found with terpenes in bound form, bound content is highly dependent on β-d-glucosyltransferase (Zhang *et al.* 2017) which pattern differs from terpene synthases.

At harvest, the only indicators that showed a strong significant

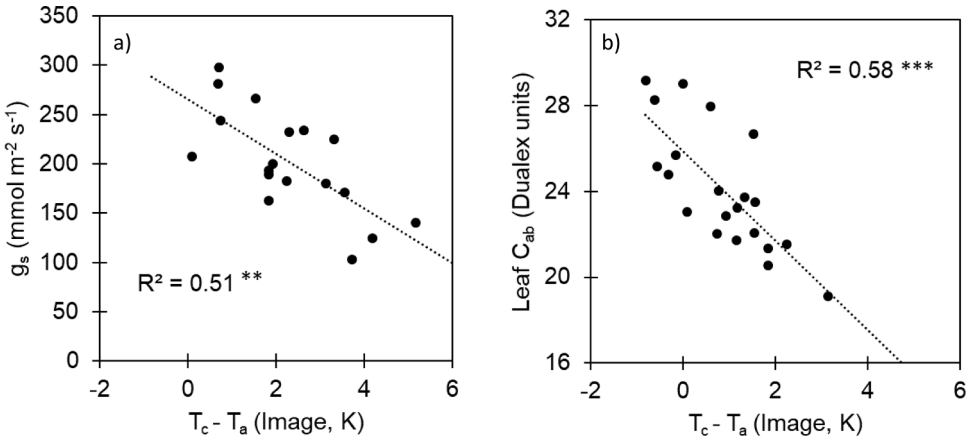

Fig. 5. Relationships between Tc-Ta derived from thermal airborne imagery and field data collected for a) stomatal conductance and b) chlorophyll content at veraison. **p-value < 0.05; **p-value < 0.01; ***p-value < 0.001; n.s.=not significant.*

Table 5
Overview of the grape composition variability across all plots.

Indicator	Mean	Minimum	Maximum	Standard deviation
Brix	27.01	23.55	31.35	1.98
pH	3.891	3.453	4.175	0.162
Colour (a.u.)	2.514	1.945	3.302	0.279
Phenolics (a.u.)	1.902	1.557	2.564	0.203
α-Terpineol (μg/kg)	1.100	0.479	1.864	0.352
Terpinolene (μg/kg)	1.043	0.436	1.731	0.397
D-Limonene (μg/kg)	0.527	0.000	1.064	0.348
β-Ionone (μg/kg)	0.004	0.001	0.006	0.001
Linalool (μg/kg)	0.276	0.094	0.471	0.087
Geraniol (μg/kg)	1.547	1.403	1.841	0.094
Nerol (μg/kg)	0.064	0.038	0.100	0.014

correlation with grape composition were the ones related to the xanthophyll pigment composition as function of stress (Table 7). In this instance, PRI, potentially affected by other pigment composition changes, did not present any correlation (Fig. 9).

The automatic segmentation of the whole vineyard allows applying the same inversion method to all vines and represent the variability of the pigment composition and stress indicators related to xanthophyll cycle activity. Fig. 10 shows the interpolated result for chlorophyll content (Fig. 10a) and carotenoid acting in photoprotection $C_{car} \bullet C_x$ (Fig. 10b) across all House Blocks after retrieving all biophysical and biochemical parameters through model inversion using pure vine spectral information.

Statistically significant relationships were found between the CWSI as an established indicator of water stress and chlorophyll $a+b$ both measured in the field and derived from model inversion, suggesting differences in water availability across the field might partially drive the existing variability in chlorophyll content. The weaker link between CWSI and grape terpene concentration as compared to the relationships obtained with pigment concentration demonstrate, though, that water stress is not the only driver of the final grape composition as shown in Fig. 11 and Tables 6 and 7.

4. Discussion

While the value of other crops is measured by biomass or fruit weight at harvest, the market value of wine grapes heavily relies on grape quality, particularly aromatic compounds which have an impact on the final quality and character of the wine produced (Yegge and Noble, 2001). The constituents that are responsible for this aromatic character are the terpenoids, unsaturated hydrocarbons with strong odours generally synthetised to attract pollinators or protect against herbivores and pathogens (Suckling *et al.*, 2012; Muhlemann *et al.*, 2014; Boachon *et al.*, 2015). There is extensive literature on the synthesis pathways of terpenes (Black *et al.*, 2015, Li *et al.*, 2020), but there are still some unknowns about the complex triggering mechanisms of such synthesis and particularly their remote detection. Imaging such compounds prior to harvest would allow prioritising and separating the outcome of blocks with more promising market value (Bramley *et al.*, 2011).

In this research, leaf pigment concentration and degradation as function of stress explained the variability found in some of the main terpenes present in the grape at harvest. The use of high-spatial resolution hyperspectral imagery allowed the automatic selection of pure sunlit vine areas avoiding known uncertainties found when using mixed vegetation-soil pixels in vineyards (Suarez *et al.*, 2010). The method used to invert plant traits through radiative transfer model inversion based on wavelet transforms was proven to retrieve plant traits accurately as can be seen in Fig. 4 and later demonstrated with the spectral fit presented in Fig. 6, for blocks with varying vigour, age and row orientation.

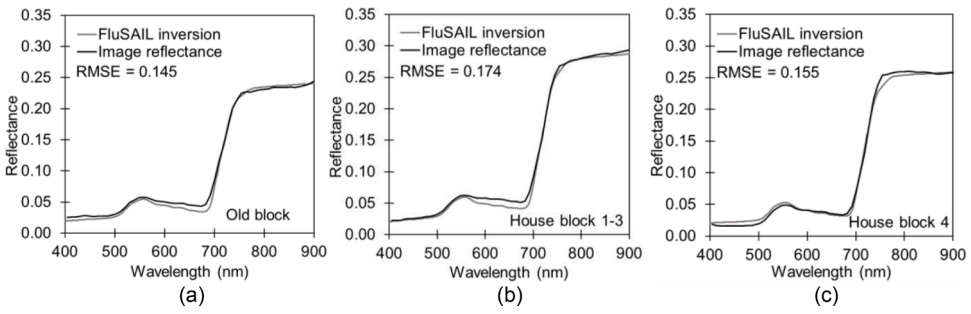

Fig. 6. Comparison between image spectra and corresponding model inversion for one of the sampling points in the Old block (a), House Blocks 1-3 (b) and House Block 4 (c).

Table 6
Pearson coefficients obtained for the correlations between spectral indices at veraison and grape composition indicators.

	Blue region indices			Green region indices related to carotenoids and photoprotection			Chlorophyll *a+b* content indices			Red-edge indices			Structural indices			Water stress
	NPQI	BF_1	BF_4	PRI	PRI/CI	CAR	T/O	LIC_3	RARS	$PSSR_c$	VOG	GM_1	CI	NDVI	RDVI	OSAVI	CWSI
°Brix	-0.12	-0.17	-0.16	0.02	-0.24	0.16	0.43	0.32	-0.26	-0.21	-0.45	-0.39	-0.45	-0.45	-0.51	-0.49	0.30
pH	-0.12	-0.04	-0.09	0.28	0.01	0.11	-0.19	0.04	-0.15	-0.14	-0.09	-0.10	-0.13	-0.27	0.03	0.13	-0.18
Colour	0.16	0.17	0.19	0.14	0.19	-0.14	-0.31	-0.17	0.17	0.18	0.28	0.20	0.23	0.10	0.17	0.18	-0.40
Phenolics	0.14	0.14	0.15	0.15	0.13	-0.08	-0.27	-0.11	0.09	0.10	0.19	0.12	0.14	-0.01	0.08	0.11	-0.34
α-Terpineol	0.26	0.37	0.37	**0.67***	0.51	-0.45	-0.44	-0.38	0.38	0.42	0.26	0.35	0.24	0.09	0.4	0.49	-0.39
Terpinolene	**-0.59***	**-0.90****	**-0.86****	**-0.81****	**-0.87****	**0.85****	**0.88****	**0.88****	**-0.75****	**-0.83****	**-0.77****	**-0.73****	**-0.72****	-0.45	**-0.59***	**-0.59***	**0.68***
D-limonene	**-0.81****	**-0.74****	**-0.87****	-0.57	**-0.79****	**0.84****	**0.75****	**0.77****	**-0.82****	**-0.82****	**-0.75****	**-0.79****	**-0.74****	**-0.61***	**-0.66***	**-0.63***	**0.70***
β-Ionone	0.36	0.47	0.45	0.14	0.32	-0.36	-0.47	-0.45	0.36	0.37	0.49	0.38	0.46	0.31	0.33	0.31	-0.24
Linalool	0.54	0.48	**0.59***	**0.63***	**0.68***	**-0.63***	**-0.64***	-0.57	**0.63***	**0.61***	0.53	**0.63***	0.52	0.41	**0.61***	**0.64***	**-0.67***
Geraniol	-0.23	-0.01	-0.13	0.32	0.10	-0.01	-0.19	-0.02	-0.23	-0.01	0.04	-0.09	-0.19	-0.20	-0.18	-0.16	-0.12
Nerol	0.13	0.32	0.27	0.42	0.26	-0.25	-0.24	-0.23	0.15	0.23	0.10	0.13	0.08	-0.04	0.17	0.23	-0.13

*p-value<0.05 **p-value<0.01

The results of the correlations between traits and grape composition demonstrate that quantitative plant traits derived from radiative transfer model inversion outperform any other method based on vegetation indices related to structure, physiology, pigment composition or pigment degradation (Tables 6 and 7). The main leaf pigment groups, chlorophylls, carotenoids and anthocyanins derived at veraison were found to explain the terpene concentration variability better than any other trait. This is in agreement with Sanchez *et al.* (2021) suggestion that foliar chlorophyll content, measured at veraison, could be a useful tool in precision viticulture for the early characterisation of the grape aromatic potential. At the same time, the degradation of chlorophyll into secondary pigments has been related to the plant defence mechanisms to the attack of pests (Barnes et al., 1992; Peñuelas et al., 1995) and the same process involves the synthesis of terpenes (Howe and Jander, 2008). Although vegetation indices commonly used to assess chlorophyll concentration presented significant relationships with terpene concentration, they did not achieve equivalent results to the ones with chlorophyll content quantified through model inversion (Fig. 7).

The link between carotenoids, including xanthophylls and terpenes is direct as they share biosynthetic pathways (Black *et al.*, 2015). Carotenoids presented a very high correlation to chlorophyll, explaining both pigment groups showing very similar results against terpinolene, D-limonene and linalool (Table 7). The role of carotenoids in grape berries has been found to be more similar to that of leaves as opposed to other crops where they play a major role in the skin colour of ripe fruits (Lin *et al.*, 2019). During berry ripening, there is a simultaneous decrease in carotenoid content and increase in norisoprenoid which are carotenoids derivatives contributing to the aroma in wine grapes. Previous studies have also linked the illumination intensity and spectrum to the final terpene composition (Carbonell-Bejarano *et al.*, 2014), which directly links the photoprotective processes to the synthesis of linalool and other terpenes (Peñuelas and Llusia, 2002; Joubert *et al.*, 2016). Xanthophyll pigment composition varies with changing light intensity to protect the photosystems from oxidative damage (Demmig-Adams and Adams, 1996). C_x is an indicator of the xanthophylls that are partly dissipating the incoming radiation as to the total carotenoid concentration. Both C_x and the product $C_{car}\bullet C_x$ was found to track the variability of α-terpineol, terpinolene, linalool and nerol at veraison (Table 7). Fig. 8 and Table 6 show how spectral indices like PRI, developed to assess xanthophyll composition dynamics did not achieve the same, potentially due to the effects of canopy structure, varying row orientation and illumination geometry on the index (Suarez *et al.*, 2008; Suarez *et al.*, 2010).

Leaf pigment composition at harvest did not show any correlation with aromatic components in the grapes. It is known there is an abrupt change in the chlorophylls and carotenoids pigment pools towards senescence (Filimon *et al.*, 2016). Chlorophyll content derived from model inversion at harvest was at average, 15 μg/cm^2 lower than at veraison, while anthocyanin content increased by 2 μg/cm^2 on average (data not shown). The results in Table 7 show the pigment concentration derive at harvest was not correlated to the variability found in the grape terpene concentration. On the other hand, C_x and $C_{car}\bullet C_x$ was found to correlate with Terpinolene, Limonene and β-Ionone, the latter being a direct subproduct of zeaxanthin degradation (Black *et al.*, 2015). Weaker correlations were found with other norisoprenoids, which might be due to the activation of individual enzymes associated with their biosynthesis. This is very common as different norisoprenoids have different accumulation pattern during ripening (Luo *et al.* 2019). Although the major leaf pigment pools at harvest were not providing much information about the grape aromatic parameters, plant traits related to photosynthetic efficiency did. Vegetation indices like PRI used as a proxy of the xanthophyll composition did not yield any good correlation (Fig. 9).

The availability of water during the grape growing period has been related in the past to final composition (Serrano *et al.*, 2012). Here we assessed the impact of water stress on the final grape composition using

Table 7
Pearson coefficients obtained for the correlations between biophysical and biochemical properties derived from FluSAIL model inversion and grape composition indicators.

	Veraison							Harvest						
	C_{ab}	C_{ant}	C_{car}	C_x	C_{car}•C_x	C_{dm}	LAI	C_{ab}	C_{ant}	C_{car}	C_x	C_{car}•C_x	C_{dm}	LAI
°Brix	-0.35	0.12	-0.44	-0.15	-0.30	0.23	-0.27	-0.28	0.20	0.32	-0.16	-0.07	0.00	-0.18
pH	0.17	-0.19	0.28	0.38	0.42	-0.04	-0.08	0.01	-0.22	-0.21	-0.35	-0.41	-0.29	-0.09
Colour	0.27	-0.44	0.28	0.00	0.12	-0.13	-0.18	-0.30	-0.28	-0.02	-0.31	-0.34	0.28	-0.13
Phenolics	0.24	-0.46	0.25	0.03	0.13	-0.21	-0.21	-0.02	-0.33	0.06	-0.34	-0.34	-0.10	0.15
α-Terpineol	0.52	-0.52	0.47	**0.80****	**0.85****	0.25	-0.51	0.17	0.20	0.23	0.09	0.15	-0.10	-0.11
Terpinolene	**-0.91****	**0.91****	**-0.78****	-0.34	**-0.61***	-0.42	0.39	0.03	-0.53	0.44	**-0.71****	**-0.61***	-0.30	0.34
D-Limonene	**-0.91****	**0.85****	**-0.85****	-0.26	-0.57	-0.34	0.13	-0.14	-0.25	0.53	**-0.55***	-0.42	0.04	0.07
β-Ionone	0.46	**-0.65***	0.40	-0.11	0.08	-0.19	-0.04	-0.08	-0.53	-0.32	**-0.61***	**-0.72****	-0.10	0.23
Linalool	**0.77****	**-0.58***	**0.79****	**0.58***	**0.81****	0.40	-0.17	0.16	-0.14	-0.24	-0.31	-0.39	-0.34	-0.07
Geraniol	0.06	-0.05	-0.07	0.09	0.06	-0.03	-0.34	0.12	**-0.58***	0.10	0.15	-0.26	-0.26	0.13
Nerol	0.26	-0.41	0.17	**0.62***	0.26	-0.20	-0.53	0.36	0.11	0.39	-0.11	0.36	-0.41	0.19

*p-value<0.05; **p-value<0.01

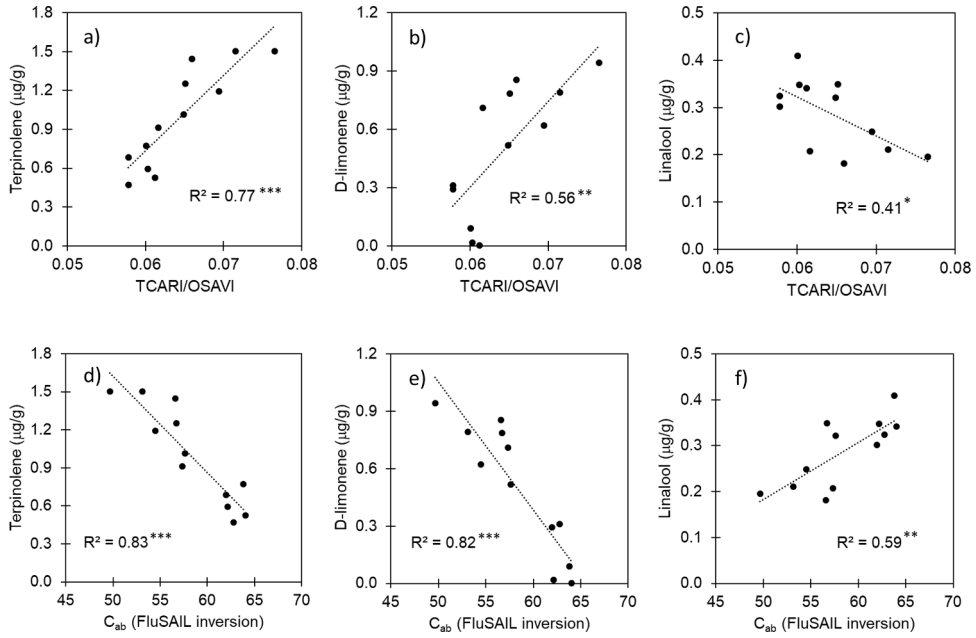

Fig. 7. Relationships found between TCARI/OSAVI as a chlorophyll indicator versus three terpenes (a-c) compared to chlorophyll content derived from model inversion versus the same terpenes (d-f) at veraison. **p-value < 0.05; **p-value < 0.01; ***p-value < 0.001; n.s.=not significant.*

the CWSI. The CWSI has been demonstrated to be a robust indicator of water stress across species (Berni *et al.*, 2009; Gonzalez-Dugo *et al.*, 2020) being an indicator used to monitor and assist irrigation management in vineyards (Bellvert *et al.*, 2015). For this study, we used the baseline equations by Bellvert *et al.* (2014) for grapes of variety shiraz. We found temperature and the CWSI to be highly correlated to leaf conductance measured in the field (r^2=0.51, p-value= 0.002) as an indicator of water stress and chlorophyll (r^2= 0.58, p-value= 6E-5) indicating water stress is one of the drivers of pigment variability in the vineyard (Fig. 5). These results were further supported by the significant relationships found between the CWSI and pigment concentrations measured in the field and derived from RTM inversion (r^2= 0.51 – 0.58, p-value= 1E-9 – 6E-5, Figs. 5 & 11). The CWSI could not, though, fully explain the variability in grape composition, as indicated in Fig. 11. These results suggest that, although the variable water availability and water stress suffered during the fruit growing period is partially driving leaf pigment concentrations and plant physiological processes affecting terpene synthesis, there are other factors contributing to the final grape composition.

Sensor and platform advancements allowing the acquisition of high-spatial and spectral resolution provide the means to assess and map vineyard areas with special characteristics that may lead to signature grape aromatic compounds resulting in added value for the wine market. Previous studies have demonstrated how important it is to select pure sunlit canopy spectra for the accurate retrieval of plant photosynthetic traits such as pigments (Zarco-Tejada *et al.*, 2013) or pigment degradation processes related to stress (Suarez *et al.*, 2010). Light hyperspectral sensors like the Nano Hyperspec can be flown using drones flying at low altitudes providing resolutions ~ 20cm/px and allowing the extraction of pure sunlit vine spectra. Here we demonstrate how this

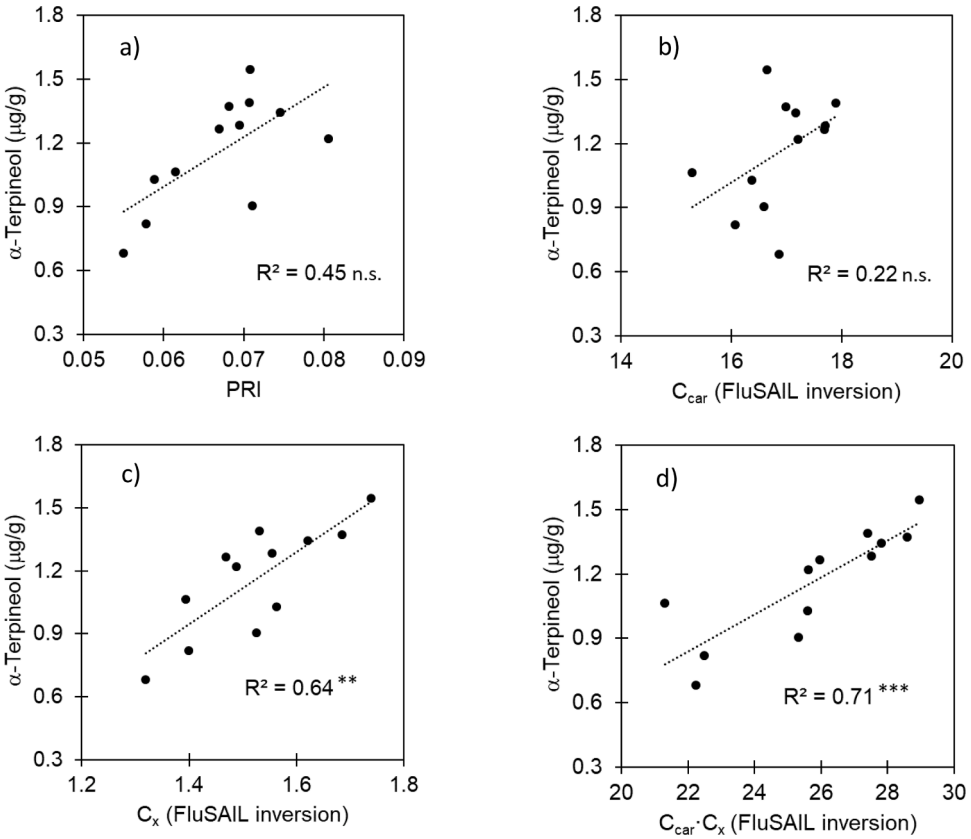

Fig. 8. Relationship between α-Terpineol and PRI as a spectral indicator of the xanthophyll composition changes under stress (a), α-Terpineol and total carotenoid content (b) and α-Terpineol with C_x (c) and C_{car}•C_x (d) derived from FluSAIL model inversion. *p-value<0.05; **p-value<0.01; ***p-value<0.001; n.s.= not significant.

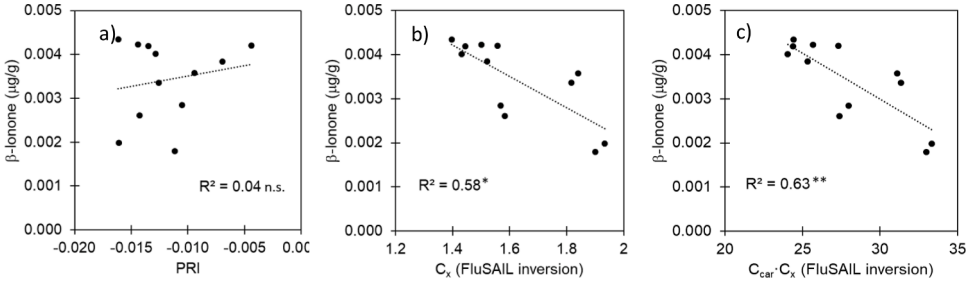

Fig. 9. Relationship between β-Ionone, sub-product of the photoprotective xanthophyll zeaxanthin and PRI as spectral indicator of the xanthophyll photoprotection state (a), C_x as the proportion of carotenoids acting in the photoprotection mechanisms (b) and the total carotenoid content acting in the photoprotection mechanism calculated as C_{car}•C_x (c). **p-value < 0.05; **p-value < 0.01; ***p-value < 0.001; n.s.=not significant.*

image acquisition settings allow the accurate mapping of vine properties over full blocks and map the spatial variability of traits that are later on related to grape quality. Variability maps can then be used to plan selective harvest operations based on spatially explicit information on grape composition and potentially added value to the final product even when production is geared to large volumes (Bramley *et al.*, 2011).

5. Conclusion

In this study we show how leaf pigment composition and dynamics as function of stress could explain the variability in aroma components in a commercial vineyard (cv. shiraz). Chlorophyll, carotenoid and anthocyanin content derived from radiative transfer model inversion at veraison outperformed traditional techniques based on vegetation indices to track grape composition. The fraction of carotenoids acting in photoprotective mechanisms under stress was highly correlated to specific terpenes measured in the grape. This work advances the detection of fruit quality, establishing the links between grape aroma components and plant traits, demonstrating their accurate detection in vineyards. We show how mapping wine grape quality is achievable through physical modelling inversion using very-high spatial resolution hyperspectral imagery, allowing the selective harvest of vineyard areas resulting in added wine character and value in the market.

Declaration of Competing Interest

The authors declare that they have no known competing financial interests or personal relationships that could have appeared to influence the work reported in this paper.

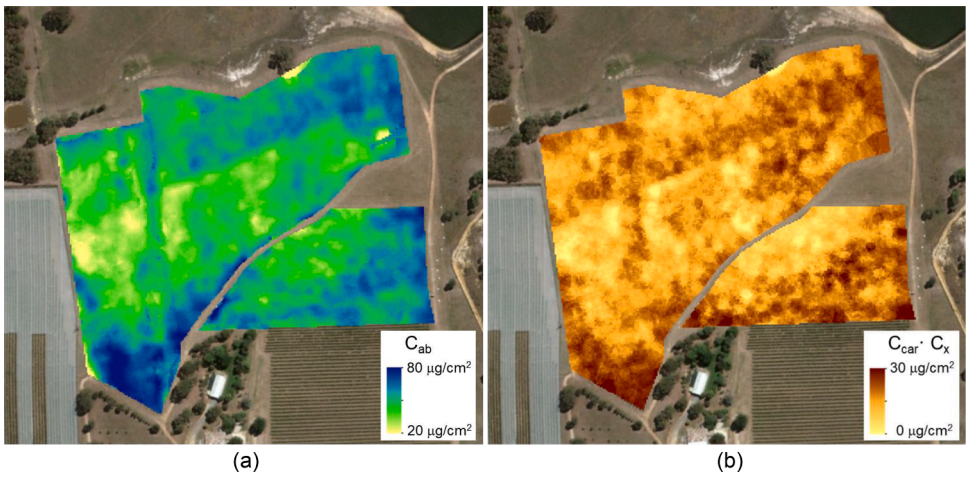

Fig. 10. Chlorophyll and C_{car}•C_x variability maps derived from FluSAIL model inversion over the House block regions.

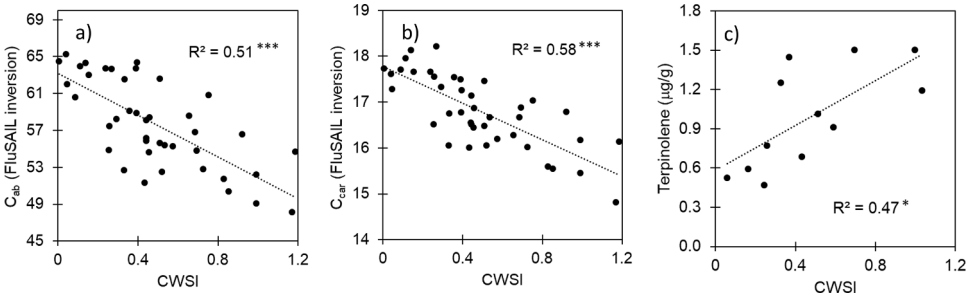

Fig. 11. Relationships obtained between CWSI and pigment content derived from model inversion (a and b). Relationship between CWSI and Terpinolene (c), one of the terpenes included in the analysis. **p-value < 0.05; **p-value < 0.01; ***p-value < 0.001; n.s.=not significant.*

Acknowledgements

The authors would like to acknowledge Damien Sheehan and the team in Mt Langi Ghiran for allowing this research to be conducted there. Chemical analysis was partially funded by the Masters Major Project program at the School of Agriculture and Food, the University of Melbourne. Rafael Romero from QuantaLab-IAS-CSIC laboratory (Spain) for data processing, and Aaron Correra, Daniel Thomas and Luke Annels from XM2 Pursuit are also acknowledged for the image data collection and participation in the airborne campaigns.

References

Barnes, J.D., Balaguer, L., Manrique, E., Elvira, S., Davison, A.W., 1992. A Reappraisal of the Use of Dmso for the Extraction and Determination of Chlorophylls-a and Chlorophylls-B in Lichens and Higher-Plants. Environ. Exp. Bot. 32 (2), 85–100.

Bellvert, J., Marsal, J., Girona, J., Zarco-Tejada, P.J., 2014. Seasonal evolution of crop water stress index in grapevine varieties determined with high-resolution remote sensing thermal imagery. Irrig. Sci. 33, 81–93. https://doi.org/10.1007/s00271-014-0456-y.

Bellvert, J., Zarco-Tejada, P.J., Marsal, J, Girona, J., González-Dugo, V., Fereres, E., 2015. Vineyard irrigation scheduling based on airborne thermal imagery and water potential thresholds. Aust. J. Grape Wine Res. 22 (2), 307–315. https://doi.org/10.1111/ajgw.12173.

Berni, J.A.J., Zarco-Tejada, P.J., Sepulcre-Cantó, G., Fereres, E., Villalobos, F.J, 2009. Mapping canopy conductance and CWSI in olive orchards using high resolution thermal remote sensing imagery. Remote Sens. Environ. 113, 2380–2388.

Black, C.A., Parker, M., Siebert, T.E., Capone, D.L., Francis, I.L., 2015. Terpenoids and their role in wine flavour: recent advances. Aust. J. Grape Wine Res. 21, 582–600.

Blackburn, G.A., 1998. Spectral indices for estimating photosynthetic pigment concentrations: A test using senescent tree leaves. Int. J. Remote Sens. 19 (4), 657–675. https://doi.org/10.1080/014311698215919.

Blackburn, G.A., 2006. Hyperspectral remote sensing of plant pigments. J. Exp. Bot. 58 (4), 855–867.

Blackburn, G.A., 2007. Hyperspectral remote sensing of plant pigments. J. Exp. Bot. 58 (4), 855–867.

Blackburn, G.A., Ferwerda, J.G., 2008. Retrieval of chlorophyll concentration from leaf reflectance spectra using wavelet analysis. Remote Sens. Environ. 112, 1614–1632.

Boachon, B., Junker, R.R., Miesch, L., Bassard, J-E, Hoefer, R., Caillieaudeaux, R., Seidel, D.E., Lesot, A., Heinrich, C., Ginglinger, J-F., Allouche, L., Vincent, B., Wahyumi, D.S.C., Paetz, C., Beran, F., Miesch, M., Schneider, B., Leiss, K., Werck-Reichhart, D, 2015. CYP76C1 (cytochrome P450)-mediated linalool metabolism and the formation of volatile and soluble linalool oxides in Arabidopsis flowers: a strategy for defense against floral antagonists. Plant Cell. 27, 2972–2990.

Boss, P.K., Kalua, C.M., Nicholson, E.L., Maffei, S.M., Bottcher, C., Davies, C., 2018. Fermentation of grapes throughout development identifies stages criticalto the development of wine volatile composition. Aust. J. Grape Wine Res. 24, 24–37.

Bramley, R., Ouzman, J., Thornton, C., 2011. Selective harvesting is a feasible and profitable strategy even when grape and wine production is geared towards large fermentation volumes. Aust. J. Grape Wine Res. 17 (3), 298–305. https://doi.org/10.1111/j.1755-0238.2011.00151.x.

Bureau, S.M., Baumes, R.L., Razungles, A.J., 2000a. Effects of vine or bunch shading on the glycosylated flavor precursors in grapes of Vitis vinifera L. Cv. Syrah. J. Agric. Food Chem. 48, 1290–1297.

Bureau, S.M., Razungles, A.J., Baumes, R.L., 2000b. The aroma of Muscat of Frontignan grapes: effect of the light environment of vine or bunch on volatiles and glycoconjugates. J. Sci. Food Agric. 80, 2012–2020.

Carbonell-Bejerano, P., Diago, MP., Martínez-Abaigar, J., Martinez-Zapater, J.M., Tardaguila, J., Nuñez-Olivera, E., 2014. Solar ultraviolet radiation is necessary to enhance grapevine fruit ripening transcriptional and phenolic responses. BMC Plant Biol. 14, 183. https://doi.org/10.1186/1471-2229-14-183 (2014).

Chappelle, E.W., Kim, M.S., McMurtrey, J.E., 1992. Ratio analysis of reflectance spectra (RARS): an algorithm for the remote estimation of the concentrations of chlorophyll a, chlorophyll b, and carotenoids in soybean leaves. Rem. Sens. Environ. 39, 239–247.

Cheng, T., Rivard, B., Sanchez-Azofeifa, A., 2011. Spectroscopic determination of leaf water content using continuous wavelet analysis. Remote Sens. Environ. 115, 659–670.

Croft, H., Chen, J.M., Zhang, Y., 2014. The applicability of empirical vegetation indices for determining leaf chlorophyll content over different leaf and canopy structures. Ecol. Complex. 17, 119–130.

Demmig-Adams, B., Adams, W.W., 1992. Photoprotection and other responses of plants to high light stress. Annu. Rev. Plant Physiol. Plant Mol. Biol. 43, 599–626.

Demmig-Adams, B., Adams, W.W., 1996. The role of xanthophyll cycle carotenoids in the protection of photosynthesis. Trends Plant Sci. 1, 21–26.

Filimon, R.V., Rotaru, L., Filimon, R.M., 2016. Quantitative investigation of leaf photosynthetic pigments during annual biological cycle of Vitis vinifera L. table grape cultivars. S. Afr. J. Enol. Vitic. 37 (1), 1–14.
Gamon, J., Penuelas, J.A., Field, C.B., 1992. A narrow-waveband spectral index that tracks diurnal changes in photosynthetic efficiency. Remote Sens. Environ. 41, 35–44.
Garrity, S.R., Eitel, J.U.H., Vierling, L.A, 2011. Disentangling the relationships between plant pigments and the photochemical reflectance index reveals a new approach for remote estimation of carotenoid content. Remote Sens. Environ. 115 (2), 628–635.
Gil-Pérez, B., Zarco-Tejada, P.J., Correa-Guimaraes, A., Relea-Cangas, E., Navas-Gracia, L.M., Hernández-Navarro, S., Sanz-Requena, J.F., Berjón, A., Martín-Gil, J., 2010. Remote sensing detection of nutrient uptake in vineyards using narrow-band hyperspectral imagery. Vitis 49 (4), 167–173.
Gil, M., Bottini, R., Berli, F., Pontin, M., Silva, M.F., Piccoli, P., 2013. Volatile organic compounds characterized from grapevine (Vitis vinifera L. cv. Malbec) berries increase at pre-harvest and in response to UV-B radiation. Phytochemistry 96, 148–157. https://doi.org/10.1016/j.phytochem.2013.08.011.
Gilmore, AM., 1997. Mechanistic aspects of xanthophyll cycle-dependent photoprotection in higher plant chloroplasts and leaves. Physiol. Plant 99, 197–209.
Gitelson, A.A., Merzlyak, M.N., 1997. Remote estimation of chlorophyll content in higher plant leaves. Int. J. Remote Sens. 18 (12), 2691–2697. https://doi.org/10.1080/014311697217558.
Gladstones, J.S., 2005. In: Dry, P.R., Coombe, B.G. (Eds.), Viticulture, 2nd edition, 190-118. Winetitles, Adelaide.
Gonzalez-Barreiro, C., Rial-Otero, R., Cancho-Grande, B., Simal-Gandara, J., 2015. Wine aroma compounds in grapes: a critical review. Crit. Rev. Food Sci. Nutr. 55, 202–218.
Gonzalez-Dugo, V., Zarco-Tejada, P.J., Intrigliolo, D.S., Ramírez-Cuesta, J.M., 2020. Normalization of the Crop Water Stress Index to Assess the Within-Feld Spatial Variability of Water Stress Sensitivity. Springer, Precis. Agric.. https://doi.org/10.1007/s11119-020-09768-6
Gonzalez-Flor, C., Serrano, L., Gorchs Altarriba, G., 2012. Predicting berry quality Attributes in cv. Xarel•lo Rain-Fed vineyards using narrow-band reflectance-based indices. Am. J. Enol. Vitic. 64, 88–97.
Haboudane, D., Miller, J.R., Tremblay, N., Zarco-Tejada, P.J., Dextraze, L., 2002. Integrated narrow-band vegetation indices for prediction of crop chlorophyll content for application to precision agriculture. Remote Sens. Environ. 81, 416–426.
Hall, A., Lamb, D.W., Holzapfel, P., Louis, J.P., 2010. Within-season temporal variation in correlations between vineyard canopy and winegrape composition and yield. Precis. Agric. 12, 103–117.
Hernandez-Orte, P., Concejero, B., Astrain, J., Lacau, B., Cacho, J., Ferreira, V., 2014. Influence of viticulture practices on grape aroma precursors and their relation with wine aroma. J. Sci. Food Agric. 95, 688–701.
Hörtensteiner, S., Kräutler, B., 2011. Chlorophyll breakdown in higher plants. Biochim. Biophys. Acta 1807, 977–988. https://doi.org/10.1016/j.bbabio.2010.12.007.
Howe, G.A., Jander, G., 2008. Plant immunity to insect herbivores. Annu. Rev. Plant Biol. 59, 41–66.
Hunter, J.J., de Villiers, O.T., Watts, J.E., 1991. The effect of partial defoliation on quality characteristics of vitis vinifera L. cv. Cabernet Sauvignon Grapes. II. skin color, skin sugar, and wine quality. Am. J. Enol. Vitic. 42 (1), 13–18.
Idso, SB, Jackson, RD, Pinter, PJ, Reginato, RJ, Hatfield, JL, 1981. Normalizing the stress-degree day parameter for environmental variability. Agric. Meteorol. 24, 45–55.
Iland, P., 2004. Chemical Analysis of Grapes and Wine: Techniques and Concepts. Patrick Iland Wine Promotions, Campbelltown, SA.
Jackson, RD, Idso, SB, Reginato, R, Pinter, PJ, 1981. Canopy temperature as a drought stress indicator. Water Resour. Res. 17, 1133–1138.
Jackson, D.I., Lombard, P.B., 1993. Environmental and management practices affecting grape composition and wine quality- a review. Am. J. Enol. Vitic. 44 (4), 409–430.
Jacquemoud, S., Verhoef, W., Baret, W., Bacour, C., Zarco-Tejada, P.J., Asner, G.P., François, C., Ustin, S.L., 2009. PROSPECT+SAIL models: a review of use for vegetation characterization. Remote Sens. Environ. 113, S56–S66.
Joubert, C., Young, P.R., Eyeghe-Bickong, H.A., Vivier, M.A., 2016. Field-grown grapevine berries use carotenoids and the associated xanthophyll cycles to acclimate to UV exposure differentially in high and low light (shade) conditions. Front. Plant Sci. 10 https://doi.org/10.3389/fpls.2016.00786.
Kattenborn, T., Fassnacht, F.E., Pierce, S., Lopatin, J., Grim, J.P., Schmidtlein, S., 2017. Linking plant strategies and plant traits derived by radiative transfer modelling. J. Veg. Sci. 28, 717–727.
Lamb, D.W., Weedon, M.M., Bramley, R.G.V, 2004. Using remote sensing to predict grape phenolics and colour at harvest in a Cabernet Sauvignon vineyard: Timing observations against vine phenology and optimising image resolution. Aust. J. Grape Wine Res. 10, 46–54.
Learned, R.M., Connolly, E.L., 1997. Light modulates the spatial patterns of 3-hydroxy-3-methylglutaryl coenzyme A reductase gene expression in Arabidopsis thaliana. Plant J 11, 499–511.
Li, Z., Howell, K., Fang, Z., Zhang, P., 2020. Sesquiterpenes in grapes and wines: Occurrence, biosynthesis, functionality, and influence of winemaking processes. Compr Rev Food Sci F 19 (1), 247–281. https://doi.org/10.1111/1541-4337.12516.
Lichtenthaler, H.K., 1999. The 1-deoxy-D-xylulose-5-phosphate pathway of isoprenoid biosynthesis in plants. Annu. Rev. Plant Physiol. Plant Mol. Biol. 50, 47–65.
Lin, J., Massonet, M., Cantu, D., 2019. The genetic basis of grape and wine aroma. Hortic. Res. 6, 81. https://doi.org/10.1038/s41438-019-0163-1.
Luo, J., Brotchie, J., Pang, M., Marriott, P. J., Howell, K., & Zhang, P. (2019). Free terpene evolution during the berry maturation of five Vitis vinifera L. cultivars. Food Chem., 125101. doi:10.1016/j.foodchem.2019.125101.
Marais, J., 1983. Terpenes in the aroma of grapes and wines: a review. S. Afr. J. Enol. Vitic. 4 (2), 49–58.
Matile, P., Hoertensteiner, S., Thomas, H., 1999. Chlorophyll degradation. Annu. Rev. Plant Physiol. Plant Mol. Biol. 50, 67–95.
Meggio, F., Zarco-Tejada, P.J., Núñez, L.C., Sepulcre-Cantó, G., Gonzalez, M.R., Martin, P., 2010. Grape quality assessment in vineyards affected by iron deficiency chlorosis using narrow-band physiological remote sensing indices. Remote Sens. Environ. 114, 1968–1986.
Mele, M.A., Kang, H.-M., Lee, Y.-T., Islam, M.Z., 2020. Grape terpenoids: flavor importance, genetic regulation, and future potential. Crit. Rev. Food Sci. Nutr. 1–19. https://doi.org/10.1080/10408398.2020.1760203.
Mittermayr, C.R., Tan, H.W., Brown, S.D., 2001. Robust calibration with respect to background variation. Appl. Spectrosc. 55, 827–833.
Muhlemann, J.K., Klempien, A., Dudareva, N., 2014. Floral volatiles: From biosynthesis to function. Plant Cell Environ. 37, 1936–1949.
Peñuelas, J., Filella, I., LLoret, P., Muñoz, F., Vilajeliu, M., 1995. Refectance assessment of mite efects on apple trees. Int. J. Remote Sen. 16, 2727–2733.
Peñuelas, J., Llusia, J., 2002. Linking photorespiration, monoterpenes and thermotolerance in Quercus. New Phytol. 155 (2), 227–237.
Rondeaux, G., Steven, M., Baret, F., 1996. Optimization of soil-adjusted vegetation indices. Remote Sens. Environ. 55, 95–107.
Rougean, J.L., Breon, F.M., 1995. Estimating PAR absorbed by vegetation from bidirectional reflectance measurements. Remote Sens. Environ. 51, 375–384.
Sánchez, R., Gonzalez García, M., Vilanova, M., Rodríguez-Nogales, J.M., Martín, P., 2021. Aroma composition of Tempranillo grapes as affected by iron deficiency chlorosis and vine water status. Sci. Agric. 78 (2), e20190112 https://doi.org/10.1590/1678-992x-2019-0112. Epub April 17, 2020.
Sasaki, K., Takase, H., Matsuyama, S., Kobayashi, H., Matsuo, H., Ikoma, G., Takata, R., 2016. Effect of light exposure on linalool biosynthesis and accumulation in grape berries. Biosci. Biotechnol. Biochem. 80 (12), 2376–2382.
Scarlett, N.J., Bramley, R.G.V., Siebert, T.E, 2014. Within-vineyard variation in the 'pepper' compound rotundone is spatially structured and related to variation in the land underlying the vineyard. Aust. J. Grape Wine Res. 20 (2), 214–222. https://doi.org/10.1111/ajgw.12075.
Schreier, P., 1979. Flavor composition of wines: a review. CRC Crit. Rev. Food Sci. Nutr. 12, 59–111.
Serrano, L., Gonzalez-Flor, C., Gorchs, G., 2012. Assessment of grape yield and composition using the reflectance based Water Index in Mediterranean rainfed vineyards. Remote Sens. Environ. 118, 249–258.
Sibson, R., 1981. A brief description of natural neighbor interpolation. In: Interpolating Multivariate Data, 1981. John Wiley & Sons, New York, pp. 21–36.
Stergios, B.G., Howell, G.S., 1977. Effects of defoliation, trellis height, and cropping stress on cold hardiness of Concord grapevines. Am. J. Enol. Vitic. 28, 34–42.
Soares Galvão, L., Marcelo Breunig, F., Sousa Teles, T., Gaida, W., Balbinot, R., 2016. Investigation of terrain illumination effects on vegetation indices and VI-derived phenological metrics in subtropical deciduous forests. GeoSci. Remote Sens. 53 (3), 360–381.
Suárez, L., Zarco-Tejada, P.J., Sepulcre-Cantó, G., Pérez-Priego, O., Miller, J.R., Jiménez-Muñoz, J.C., Sobrino, J., 2008. Assessing Canopy PRI for Water Stress detection with Diurnal Airborne Imagery. Remote Sens. Environ. 112, 560–575.
Suárez, L., Zarco-Tejada, P.J., Berni, J.A.J., González-Dugo, V., Fereres, E., Goldhamer, D, 2010. The effect of spatial resolution in remote sensing of water stress using optical and thermal imagery. In: 3rd International Symposium Recent Advances in Quantitative Remote Sensing, 27th September-1st October 2010, ISBN: 978-84-370-7952-3. Publicacions de la Universitat de Valencia, Valencia, Spain, pp. 355–357.
Suárez, L., Zarco-Tejada, P.J., González-Dugo, V., Berni, J.A.J., Sagardoy, R., Morales, F., Fereres, E, 2010. Detecting water stress effects on fruit quality in orchards with time-series PRI airborne imagery. Remote Sens. Environ. 114, 286–298.
Suárez, L., Gonzalez-Dugo, V., Camino, C., Hornero, A., Zarco-Tejada, P.J., 2021. Physical model inversion of the green spectral region to track assimilation rate in almond trees with an airborne nano-hyperspectral imager. Remote Sens. Environ. 252, 112147 https://doi.org/10.1016/j.rse.2020.112147.
Suckling, D.M., Twidle, A.M., Gibb, A.R., Manning, L.M., Mitchell, V.J., Sullivan, T.E.S., Wee, S.L., El-Sayed, A.M., 2012. Volatiles from appletrees infested with light brown apple moth larvae attract the parasitoid Dolichogenidia tasmanica. J. Agric. Food Chem. 60, 9562–9566.
Šuklje, K., Antalick, G., Coetzee, Z., Schmidtke, L.M., Baša Česnik, H., Brandt, J., du Toit, W.J., Lisjak, K., Deloire, A., 2014. Effect of leaf removal and ultraviolet radiation on the composition and sensory perception of Vitis vinifera L. cv. Sauvignon Blanc wine. Aust. J. Grape Wine Res. 20 (2), 223–233. https://doi.org/10.1111/ajgw.12083.
Torrence, C., Compo, G., 1998. A practical guide to wavelet analysis. Bull. Am. Meteorol. Soc. 79, 61–78.
Van der Tol, C., Verhoef, W., Timmermans, J., Verhoef, A., Su, Z., 2009. An integrated model of soil-canopy spectral radiances, photosynthesis, fluorescence, temperature and energy balance. Biogeosciences 6 (12), 3109–3129.
Verhoef, W., 1984. Light scattering by leaf layers with application to canopy reflectance modeling: the SAIL model. Remote Sens. Environ. 16, 125–141.
Verhoef, W., Xiao, Q., Jia, L., Su, Z., 2007. Unified optical-thermal four-stream radiative transfer theory for homogeneous vegetation canopies. IEEE Trans. Geosci. Remote Sens. 45, 1808–1822.
Vilfan, N., Van der Tol, C., Muller, O., Rascher, U., Verhoef, W., 2016. Fluspect-B: amodel for leaffluorescence, reflectanceand transmittance spectra. Remote Sens.Environ. 186, 596–615.

Vilfan, N., Van der Tol, C., Yang, P., Wyber, R., Malenovský, Z., Robinson, S.A., Verhoef, W., 2018. Extending Fluspect to simulate xanthophyll driven leaf reflectance dynamics. Remote Sens. Environ. 211, 345–356.

Vogelmann, J.E., Rock, B.N., Moss, D.M., 1993. Red Edge Spectral Measurements from Sugar Maple Leaves. Int. J. Remote Sens. 14 (8), 1563–1575.

Vranova, E., Coman, D., Gruissem, W., 2012. Structure and dynamics of the isoprenoid pathway network. Mol. Plant 5 (2), 318–333.

Yegge, J.M., Noble, A.C., 2001. The identification of sensory and non-sensory attributes of California Chardonnay wines that influence acceptance and purchase intent for differing segments of consumers. In: Proceedings of the American Society for Enology and Viticulture. Seattle, WA. American Society for Enology and Viticulture, pp. 28–31.

Yu, F., Utsumi, R., 2009. Diversity, regulation, and genetic manipulation of plant mono- and sesquiterpenoid biosynthesis. Cell. Mol. Life Sci. 66, 3043–3052.

Zarco-Tejada, P.J., Miller, J.R., Mohammed, G.H., Noland, T.L., Sampson, P.H., 2001. Scaling-up and model inversion methods with narrow-band optical indices for chlorophyll content estimation in closed forest canopies with hyperspectral data. IEEE Trans. Geosci. Remote Sens. 39 (7), 1491–1507.

Zarco-Tejada, P.J., Guillén-Climent, M.L., Hernández-Clemente, R., Catalina, A., González, M.R., Martín, P., 2013. Estimating leaf carotenoid content in vineyards using high resolution hyperspectral imagery acquired from an unmanned aerial vehicle. Agric. For. Meteorol. 171-172, 281–294.

Zarco-Tejada, P.J., Camino, C., Beck, P.S.A., Calderon, R., Hornero, A., Hernández-Clemente, R., Kattenborn, T., Montes-Borrego, M., Susca, L., Morelli, M., Gonzalez-Dugo, V., North, P.R.J., Landa, B.B., Boscia, D., Saponari, M., Navas-Cortes, J.A., 2018. Pre-visual symptoms of Xylella fastidiosa infection revealed in spectral plant-trait alterations. Nat. Plants. https://doi.org/10.1038/s41477-018-0189-7.

Zhang, E., Chai, F., Zhang, H., Li, S., Liang, Z., Fan, P., 2017. Effects of sunlight exclusion on the profiles of monoterpene biosynthesis and accumulation in grape exocarp and mesocarp. Food Chem. 237, 379–389. https://doi.org/10.1016/j.foodchem.2017.05.127, 2017 Dec 15.

Zhang, P., Fuentes, S., Siebert, T., Krstic, M., Herderich, M., Barlow, E.W.R., Howell, K, 2016. Comparison data of common and abundant terpenes at different grape development stages in Shiraz wine grapes. Data Brief 8, 1127–1136.

Zhang, Y., Migliavacca, M., Peñuelas, J., Ju, W., 2021. Advances in hyperspectral remote sensing of vegetation traits and functions. Remote Sens. Environ. 252, 112121.